

Optimization of Yield in Magnetic Cell Separations Using Nickel Nanowires of Different Lengths

Anne Hultgren,[†] Monica Tanase,[†] Edward J. Felton,[†] Kiran Bhadriraju,[‡] Aliasger K. Salem,[‡] Christopher S. Chen,[‡] and Daniel H. Reich^{*,†}

Departments of Physics and Astronomy and Biomedical Engineering, The Johns Hopkins University, Baltimore, Maryland 21218 and 21205

Ferromagnetic nanowires are shown to perform both high yield and high purity single-step cell separations on cultures of NIH-3T3 mouse fibroblast cells. The nanowires are made by electrochemical deposition in nanoporous templates, permitting detailed control of their chemical and physical properties. When added to fibroblast cell cultures, the nanowires are internalized by the cells via the integrin-mediated adhesion pathway. The effectiveness of magnetic cell separations using Ni nanowires 350 nm in diameter and 5–35 micrometers long in field gradients of 40 T/m was compared to commercially available superparamagnetic beads. The percent yield of the separated populations is found to be optimized when the length of the nanowire is matched to the diameter of the cells in the culture. Magnetic cell separations performed under these conditions achieve 80% purity and 85% yield, a 4-fold increase over the beads. This effect is shown to be robust when the diameter of the cell is changed within the same cell line using mitomycin-C.

Introduction

There are an ever-increasing variety of micron- and submicron-sized particles being explored for biological and biophysical applications. Because the geometry of these particles may have biological effects (1, 2), with implications ranging from fundamental questions of how cells respond to their physical environment to diagnostic and therapeutic applications, it is important to study the role of the particles' size and shape on the mechanism of their interactions with cells. Magnetic nanoparticles have found wide utility as a means of applying force to biological systems, with applications varying from studies of mechanotransduction at the cellular level (3) to cell separations, cancer therapy, and biosensing (4–7). Although the standard particles currently used for magnetic manipulation of cells are superparamagnetic beads, an alternative type of nanoparticle with considerable potential in this area is electrodeposited nanowires (8). These nanowires have several properties that make them attractive for biological applications. Many different materials, both magnetic and nonmagnetic, can be selectively electrodeposited along the growth axis (9). Unlike the beads, which are composed of magnetic nanoparticles dispersed in a polymer matrix, the nanowires are solid metal and hence may have large magnetic moments per volume of material that are further enhanced by their magnetic shape anisotropy, allowing large forces and torques to be applied. They can be electrodeposited in many different templates ranging from nanometer to micrometer dimensions (10–12) spanning many relevant biological length scales, and their diameter and length are independently tunable. Finally,

they are compatible with living cells as they do not disrupt normal cell functions including cell proliferation, adhesion, and gene expression, and they can be functionalized with biologically active molecules (13–15).

In previous studies of nanowire–cell interactions, we have shown that ferromagnetic Ni nanowires of length $L = 35 \mu\text{m}$ have the potential to outperform magnetic beads of comparable volume in cell separation applications (16). Here the mechanism of those interactions was explored, focusing on the effects of changing nanowire length relative to cell size in magnetic separations. After seeding nanowires over a culture of adherent NIH-3T3 cells, the cells were found to bind to the nanowires through integrin receptors, as indicated by the formation of focal adhesions along the length of the nanowires. This process occurred quickly (<1 h), and the cells were found to internalize even the largest nanowires. By 24 h, nearly all of the nanowires were internalized and appeared to be in the cytoplasm rather than in a lipid vesicle, as observed by transmission electron microscopy (TEM). Following introduction of the nanowires into the cell culture, the cells were detached from the substrate, and the suspension of cells was separated in a magnetic field. Nanowires were found to generate high-purity separations over a considerable range of nanowire sizes. Interestingly, we found that the separation yield was optimized when the nanowires' length corresponded to the average diameter of the suspended cells, indicating strong length dependence to the cell–nanowire interaction process. When the average cell diameter was changed within the same cell line, the optimal nanowire length adjusted accordingly. By performing a magnetic separation on a cell population with a bimodal size distribution, we were able to selectively capture the cells with larger diameter, suggesting the potential use of nanowires to magnetically separate cell populations by size through control of the geometry of the wires.

* To whom correspondence should be addressed. Ph: 410-516-7899. Fax: 410-516-7239. Email: dhr@pha.jhu.edu.

[†] Department of Physics and Astronomy.

[‡] Department of Biomedical Engineering.

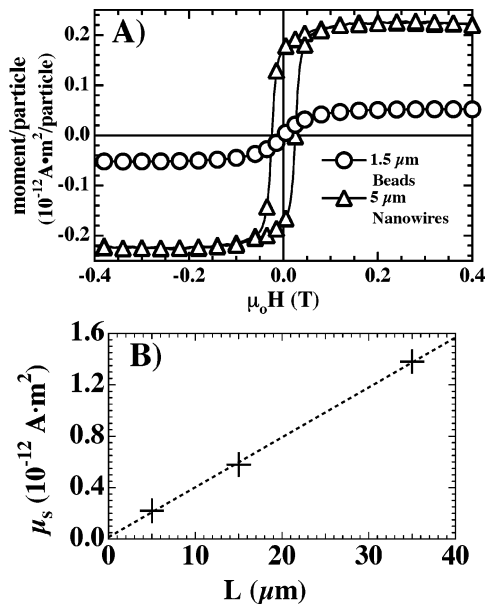


Figure 1. (A) Magnetic moment per particle versus magnetic field, $\mu_0 H$, at room temperature for beads and 5- μm nanowires. (B) Saturation moment versus nanowire length at $\mu_0 H = 0.4 \text{ T}$ and straight-line fit with slope $\mu_s/L = 3.9 \times 10^{-14} \text{ A}\cdot\text{m}^2/\mu\text{m}$.

Materials and Methods

Nanowire Fabrication. The nanowires were formed by electrochemical deposition in the pores of 50- μm -thick Anodisc (Whatman, Inc.) alumina filter templates with a nominal pore diameter of 100 nm. A 300-nm-thick copper film was sputter-coated on one side of the template to serve as the working electrode. Nickel was deposited from a solution of 20 g/L $\text{NiCl}_2\cdot 6\text{H}_2\text{O}$, 515 g/L $\text{Ni}(\text{H}_2\text{NSO}_3)_2\cdot 4\text{H}_2\text{O}$, and 20 g/L H_3BO_3 at pH 3.4, using an applied voltage of -1 V (Ag/AgCl) (17). This procedure produces an array of nickel nanowires filling the pores of the template, with the length of the nanowires determined by the deposition time. After deposition, the copper film was removed using 0.05 M CuCl in 10% HCl, and the template was dissolved in a 60 $^\circ\text{C}$, 0.5 M KOH bath, leaving the nanowires suspended in solution. Using a permanent magnet, the nanowires were immobilized against the inside wall of a flask and cleaned several times with deionized (DI) water. This process exposed the nanowires to fields in excess of 0.1 T, which is sufficient to give them their full remanent magnetization (see Figure 1A). Samples of nanowires were prepared with lengths $L = 5, 9, 15, 22,$ and $35 \mu\text{m}$ ($\pm 10\%$), all with diameter of $350 \pm 40 \text{ nm}$, as measured in a scanning electron microscope (SEM).

Cell Culture. The cells used in this study were NIH-3T3 mouse fibroblasts, obtained from the American Type Culture Collection, cultured in Dulbecco's Modified Eagle Medium (DMEM) supplemented with 5% calf serum, 100 U/mL penicillin, and 100 $\mu\text{g}/\text{mL}$ streptomycin (Gibco Life Sciences). To create cell populations with larger average volume, the cells were exposed to a solution of 10 $\mu\text{g}/\text{mL}$ of Mitomycin-C (MitoC, Sigma) in media and incubated (37 $^\circ\text{C}$, 5% CO_2) for 1 h. After treatment, the cells were washed three times with fresh media and cultured further as above.

Nanowires were sterilized in 70% ethanol/DI, transferred to culture media, and added to cultures of 3T3 cells. To test for short-term toxic effects due to the nanowires on the cells, the cell proliferation rate of samples both with and without 35- μm -long nanowires was monitored by measuring the density of the cell

populations over the course of 3 days. Images were taken with a 10X objective on a Nikon Eclipse TS100 inverted microscope over 7% of the total cell population, and the number of cells in the images was counted to determine the density.

Immunofluorescence Staining. To characterize the mechanism of cell adhesion to nanowires, cells exposed to nanowires were immunostained for both actin filaments and the focal adhesions protein paxillin. Cells were cultured on glass coverslips, incubated with nanowires for 30 min or 24 h, rinsed with $1 \times$ phosphate-buffered saline (PBS) containing 5 mM CaCl_2 and 2 mM $\text{MgCl}_2\cdot 6\text{H}_2\text{O}$, and then fixed with 4% paraformaldehyde in PBS for 15 min at room temperature. Samples were then permeabilized with 0.2% Triton-X in PBS (TPBS) for 5 min, exposed to blocking solution containing 33% goat serum in TPBS for 30 min, and then incubated with anti-paxillin mouse antibody (Transduction Laboratories) at a concentration of 2.5 $\mu\text{g}/\text{mL}$ in the blocking solution for 30 min at room temperature. Samples were rinsed in TPBS 3 times for a total time of 5 min and incubated with 1 $\mu\text{g}/\text{mL}$ of AlexaFluor-488-conjugated goat anti-mouse IgG (Molecular Probes) to bind to the paxillin sites and 0.2 U/mL TRITC-Phalloidin to bind to actin filaments in 1% BSA in TPBS for 45 min. Samples were rinsed several times with 1% BSA in TPBS before imaging with a Roper Scientific CoolSnapHQ CCD camera mounted onto a Nikon TE2000 fluorescence microscope.

Internalization Study. Nanowires, at a density of $10^6/\text{mL}$, were incubated at room temperature for 1 h in 10 $\mu\text{g}/\text{mL}$ mouse IgG in PBS. The nanowire solution was then rinsed in PBS several times and transferred into media at a density of $10^5/\text{mL}$. Cells, grown on glass coverslips, were incubated with the coated nanowires for both 30 min and 24 h. After incubation, the cells were rinsed with PBS containing 5 mM CaCl_2 and 2 mM $\text{MgCl}_2\cdot 6\text{H}_2\text{O}$, fixed with 4% paraformaldehyde in PBS for 15 min at room temperature, and rinsed again. Without permeabilizing the membrane, the mouse IgG immobilized on regions of the nanowires that were not internalized by the cells was detected with 1 $\mu\text{g}/\text{mL}$ AlexaFluor-488-conjugated goat anti-mouse IgG, and the actin was visualized by exposure to 0.2 U/mL TRITC-Phalloidin in 1% BSA in PBS for 45 min. Finally, the cells were rinsed several times with 1% BSA in PBS.

This study was repeated to determine if cells that had internalized a nanowire retained the nanowire after being suspended. Mouse IgG coated nanowires were prepared as above and added to plated cell cultures for a 24 h incubation. Glass coverslips were treated with 10 $\mu\text{g}/\text{mL}$ poly-lysine (Sigma) in sterile DI water for 1 h and rinsed several times with PBS. The cells were then suspended by exposure to $1 \times 0.25\%$ trypsin in 1mM EDTA $\cdot 4 \text{ Na}$, transferred to serum-free DMEM, plated on the poly-lysine treated coverslips, and allowed to adhere for 10 min. They were then fixed and stained as described above.

Preparation of Samples for SEM. Cells were prepared for SEM imaging by dissociating them from the culture dish with $1 \times 0.25\%$ trypsin in 1 mM EDTA $\cdot 4 \text{ Na}$, suspending them in 0.5 mL of PBS, and pipetting them onto a glass coverslip. After 1 min, they were fixed by adding an equal volume of 4% glutaraldehyde/4% paraformaldehyde in PBS and refrigerating overnight. After warming to room temperature, they were rinsed with 0.1 M calcium cacodylate with 3 mM CaCl_2 three times for 10 min each and postfixed with 2% OsO_4 in 0.1 M calcium cacodylate with 3 mM CaCl_2 for 1 h. Samples were then rinsed with distilled water twice for 5 min each and

stained with 2% uranyl acetate for 30 min. The samples were then quickly rinsed with 50% ethanol; dehydrated with 50%, 70%, and 90% ethanol for 5 min each; and dehydrated with 100% ethanol three times for 5 min each. The samples were then chromium sputter-coated.

Preparation of Samples for TEM. Cells that had been incubated with nanowires for 24 h were prepared for TEM analysis by fixing with 3% formaldehyde/1.5% glutaraldehyde in a 0.1 M sodium cacodylate solution with 2.5% sucrose at pH 7.4 for 1 h at room temperature. Samples were then rinsed in 0.1 M sodium cacodylate and 2.5% sucrose three times for 15 min each and postfixed in 0.03 M sodium acetate, 0.03 M sodium barbital, 0.02 M HCl, and 1% OsO₄ in DI for 1 h on ice in a light-tight chemical hood. They were then rinsed in 0.03 M sodium acetate, 0.03 M sodium barbital, 0.028 M HCl, and 1.2 mM uranyl acetate and incubated in the dark at room temperature overnight. The samples were then rinsed once at room temperature in DI water and quickly rinsed with 50% ethanol at 4 °C. Samples were successively dehydrated using 70%, 95%, and 100% ethanol at 4 °C, and then rinsed at room temperature with 100% ethanol three times for 15 min each and then two 5 min exchanges with propylene oxide. Samples were placed in 50% propylene oxide/50% Epon (Electron Microscopy Sciences) overnight uncovered under vacuum. The solution was replaced with 100% Epon and left under vacuum for 4–6 h. The samples were finally embedded in fresh 100% Epon using beam capsules and cured at 60 °C for 24–48 h. The samples were sectioned using a Leica Ultracut microtome into 90-nm-thick sections and mounted on copper TEM grids.

Magnetic Separations. Nanowires or magnetic beads (1.5 μm diameter, Polysciences, Inc.), which were used as a control, were added to the cell cultures. The particle solutions were first sterilized in 70% ethanol/DI water, transferred to media at a density of 6×10^5 particles/mL, and dispersed by brief ultrasonic agitation immediately prior to addition to the culture. This dispersal produces single wires in solution, and at these low concentrations the nanowires do not agglomerate significantly as a result of their remanent magnetization before settling onto the cells. To study the effectiveness of individual particles in performing cell separations, the ratio of particles to cells was kept low and ranged from 1:5 to 1:20. This limited the number of cells that were able to bind to more than one magnetic particle.

The magnetic separation device consists of two rare earth magnets (diameter = 1.3 cm) fixed on opposite sides of a 1-cm-diameter glass test tube with their poles antialigned. The magnets have a face field of 0.3 T, and together they produce an average field gradient of 40 T/m inside the test tube. A 5-min exposure to this magnetic field is sufficient to move a magnetic particle bound to a cell from the center of the tube to one of the magnets.

To perform a separation, cells that had been incubated with magnetic particles for 24 h were suspended in media using trypsin. The average initial cell density was $80,000 \pm 5,000$ cells/mL. Half of the cells were introduced into the magnetic separator, and half were replated to determine the fraction of cells bound to magnetic particles at the start of the separation. After separation, the cells that had not been captured by the magnets were extracted. The magnets were then removed, and the cells that remained in the separator were resuspended in media and plated. All populations, initial, captured, and uncaptured, were incubated for 1 h to allow the cells to settle and adhere to the dishes. Images were then taken over a 16-mm² area of each sample, covering 1% of the

total dish, using the 10X objective of a Nikon TS100 tissue culture microscope equipped with a Nikon CoolPix995 digital camera.

Separations of heterogeneous cultures of MitoC-treated and untreated cells were performed as follows. Half of the cultures were treated with MitoC 48 h prior to separation. After 24 h, the treated cells were stained red and the untreated cells were stained green using PKH26 and PKH67 general membrane marker kits (Sigma). The treated and untreated cells were then mixed to an average concentration of $7,000 \pm 1,500$ cells/mL, and 4 mL of the 9-, 15-, or 22-μm nanowire solution was added to the culture, which results in an average of 80% of the cells in the culture binding to at least one nanowire after 24 h. After separation as described above, images of the resulting cell cultures were taken in phase, brightfield, green fluorescent, or red fluorescent light using the 10X objective on a Nikon TE2000 microscope with a CoolSnapHQ camera.

Results and Discussion

Magnetic Properties of the Particles. Figure 1A shows the room-temperature magnetization curves, M vs $\mu_0 H$, for the beads and for 5-μm nanowires with $\mu_0 H$ parallel to the wire axis, measured with a vibrating sample magnetometer (VSM) as described previously (16). The beads show no remanent magnetization and have a saturation magnetization of $M_S = 32$ kA/m, consistent with the value $M_S = 35\text{--}45$ kA/m specified by the manufacturer (18). For the nanowires, the shape of the magnetization curve is nearly independent of wire length, with coercive field $\mu_0 H_C \approx 0.025$ T and remanent magnetization $M_R \approx 0.8M_S$, in agreement with previous results (8). As shown in Figure 1B, the saturation moment of the nanowires scales with their length with a slope of $\mu/L = 3.9 \times 10^{-14}$ A·m²/μm, corresponding to an average magnetization of 406 kA/m. This saturation magnetization is lower than the value of 485 kA/m for bulk nickel, possibly because of surface oxidation of the nickel nanowires during their exposure to KOH. Note that although the volume of the 35-μm nanowires is only 1.5 times the volume of the beads, their saturation moment per particle is 20 times the saturation moment of the beads. This results in a magnetic force on the nanowires in the separator that is 20 times greater than the force on the beads since the force on a particle scales with its magnetic moment. Thus, we are using particles with greatly enhanced magnetic response without increasing the amount of foreign material introduced into the cell culture.

Nanowires in Cell Culture. Two cultures of cells were prepared, one without nanowires and one in which 80% of the cells were bound to a 35-μm-long nanowire. As shown in Figure 2, the density of cells in each dish doubled every 24 h for at least 3 days. Therefore, even with nanowires bound to them, the cells were able to divide at the same rate as cells without nanowires in their culture, suggesting that the nanowires do not affect cell function at these time scales.

Previous studies have shown that fibroblast cells take up magnetic beads by first forming focal adhesions on the particles before internalization (19, 20). These focal adhesions formed by the cell during phagocytosis are specialized structures that contain high concentrations of many proteins, including among others actin and paxillin. Immunofluorescence microscopy of cells exposed to nanowires confirms that the cells also internalize the nanowires through a similar integrin-mediated phago-

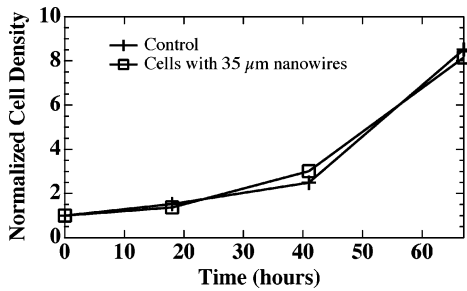


Figure 2. Normalized density of cells both with and without 35- μm nanowires versus time, showing that cells cultured with nanowires continue to divide at the same rate as the control cells.

cytosis. Cells exposed to nanowires were fixed and stained for filamentous actin and paxillin localization at various times following exposure. As seen in Figure 3A and B, the cells interact with the nanowires by forming focal adhesions along the length of the nanowire as shown by the discrete concentrations of paxillin that cluster on the nanowire. Actin is also concentrated along the length of these nanowires. At 30 min, these focal adhesions are clearly present, but they disappear within 24 h, suggesting that the cells have internalized the nanowires. To provide direct confirmation that nanowires were being internalized on this time scale, nanowires were coated with mouse IgG protein before incubation with the cells, exposed to the cells, and fixed and stained with fluorescently tagged anti-mouse antibodies. As illustrated in Figure 3C and D, after 30 min incubation with the IgG-coated nanowires, the nanowires are detected by the fluorescent anti-mouse antibody and are therefore external to the cells. However, after 24 h, the nanowires are protected from the fluorescent stain as seen in Figure 3E and F and have thus been internalized by the cells. Quantifying these results, we found that the percent of nanowires internalized increased with time from 10% at 30 min to 70% at 24 h. To further characterize which subcellular compartment the internalized nanowires were taken into, cells incubated with nanowires for 24 h were fixed, sectioned, and prepared for TEM analysis. Figure 3G is a TEM image of a cell incubated with a nanowire for 24 h, where the section has been made perpendicular to the long axis of the nanowire to show it in a cross-sectional view. The nanowires were not found with a lipid bilayer envelope, indicating that the nanowires are trafficked into the cytoplasmic compartment.

Magnetic Separations. Cells were exposed to nanowires for 24 h and suspended, and nanowire-bound cells were separated from the population using magnetic force. Images were acquired following the cell separations and analyzed to determine both the total number of cells and the number of cells attached to particles in each sample. No measurable loss of cells or cell death occurred during the separation. We compared the effectiveness of the beads and nanowires in performing cell separations using two indicators, purity and yield. The purity is defined as the percentage of cells in the captured population with a nanowire bound to them. The yield is defined as the number of captured cells with magnetic particles divided by the initial number of cells with magnetic particles. Results for the percent purity and yield of separations performed with nanowires and beads are shown in Figure 4A and B. Each result is averaged over at least four runs, and the error bars represent the standard error of the mean. The purity of the captured populations increased from below 50% for the beads and 5- μm nanowires to as high as 76% for the 35- μm nanowires. The purity was

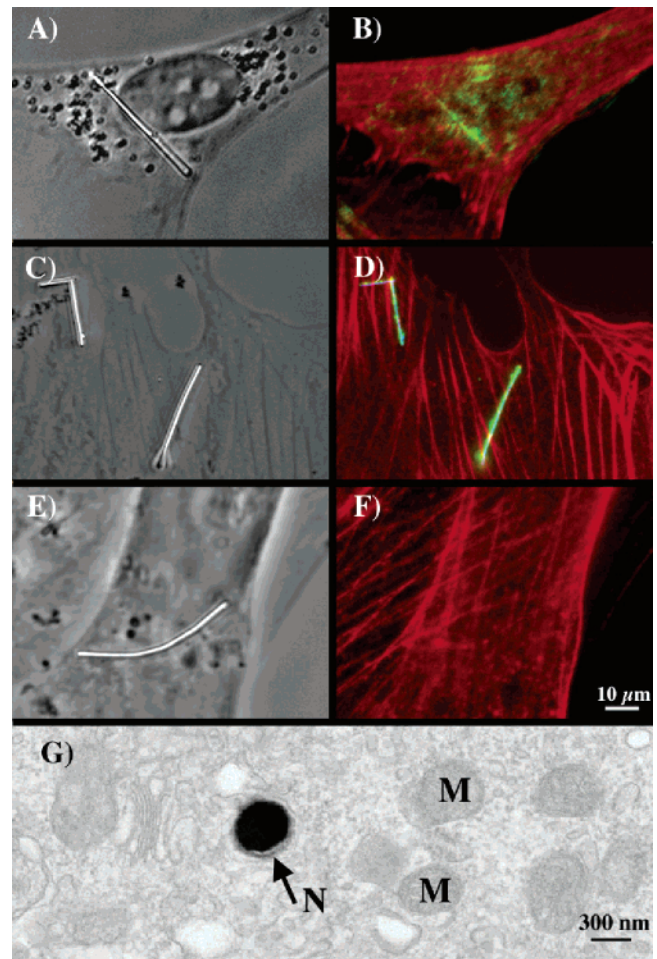


Figure 3. Binding of cell to nanowire. Top row: (A) phase contrast image of a cell incubated with a 35- μm nanowire for 30 min and (B) composite fluorescent image of the same cell showing actin filaments (red) and paxillin focal adhesions (green). Second row: (C) phase contrast image of a cell after a 30 min incubation with mouse IgG coated nanowires and (D) composite fluorescence image of the same cell showing actin filaments (red) and immunofluorescent staining of mouse IgG (green) on the nanowire, indicating that the nanowire is external to the cell. Third row: (E) phase contrast image of a cell after a 24 h incubation with mouse IgG coated nanowires and (F) composite fluorescence image of the same cell showing actin filaments (red) only. The mouse IgG on the nanowire is unstained, indicating that the nanowire is internalized. Bottom row: (G) TEM image of a cell incubated with a nanowire for 24 h; N = nanowire, M = mitochondria.

improved significantly by performing a three-pass separation, in which the separated cell population was introduced into the magnetic separator two additional times. After three passes, the beads and shorter nanowires have a purity around 86%, whereas the longer nanowires have purities up to 98%. Note that a single-pass separation with the long nanowires achieves nearly the same purity as the three-pass separation using beads.

The percentage yield increased with nanowire length for the short nanowires in single-pass separations but was found to peak at 75% when the 15- μm -long nanowires were used and then decreased sharply for the longer nanowires. This decrease in yield implies that the longer nanowires were detaching from the cells throughout the separation process, although the high purity of the captured populations using the long nanowires meant this detachment does not occur after cell capture, but instead it occurred earlier in the cell separation process. The yield decreased to below 30% for all particles using

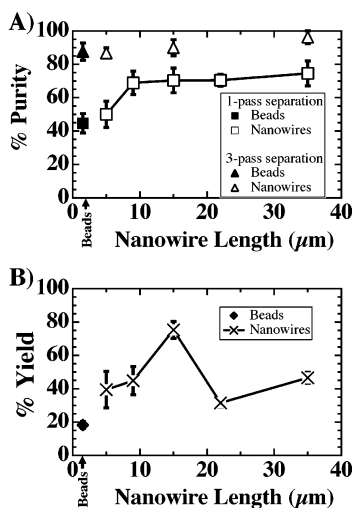


Figure 4. Percent purity versus particle size for separations using 1.5- μm beads and 5- to 35- μm nanowires in (A) both single- and three-pass separations, and (B) percent yield versus particle size for single-pass separations.

a three-pass separation process. Therefore, we were able to maximize both the purity and yield of the separated cell population by performing a single-pass separation using the 15- μm nanowires.

To investigate whether the cells were releasing the longer nanowires during the separation process, we repeated the internalization study on cells that were first incubated with IgG-coated nanowires for 24 h and then detached and suspended by exposure to trypsin. We found that because the cells in suspension form spheres, they interact with the nanowires differently depending on whether the length of the nanowire is longer or shorter than the diameter of the suspended cells. For example, Figure 5A and B are transmitted light and fluorescence images of two 9- μm nanowires, one that is freely floating and one that is attached to a suspended cell. We found that nanowires that were free from cells were stained by the dye, whereas nanowires associated with cells were protected from the fluorescent stain and hence were still internal to the cell. Therefore, when the cells were attached to nanowires with lengths smaller than their diameter, the nanowire could remain enclosed by the cell even when detached from the substrate. In contrast, as shown in Figure 5C and D, when the nanowire length was larger than the diameter of the suspended cells, the nanowire was no longer protected from the stain. We observed that 75% of the suspended cells showed fluorescence on the portion of the nanowire that appeared to be outside of the cell. However, for 25% of the suspended cells that were bound to long nanowires, the entire length of the nanowire stained. An SEM image of a 15- μm -diameter cell with a 22- μm -long nanowire is shown in Figure 5E, along with a detail of the end of the nanowire in Figure 5F, which confirms that the nanowire is external to the cell. These studies suggest that the longer nanowires are indeed protruding out of the cell, and this exposed section of the nanowire may be more susceptible to influences of mechanical stresses that could more easily remove the nanowire from the cell. This may constitute the basis for how the cells lose the long nanowires during the separation process, although further investigation of this phenomenon is necessary to reach a definitive conclusion.

To investigate whether the peak in percentage yield was influenced by the diameter of the cells or was inherent to the absolute length of the nanowires, 3T3

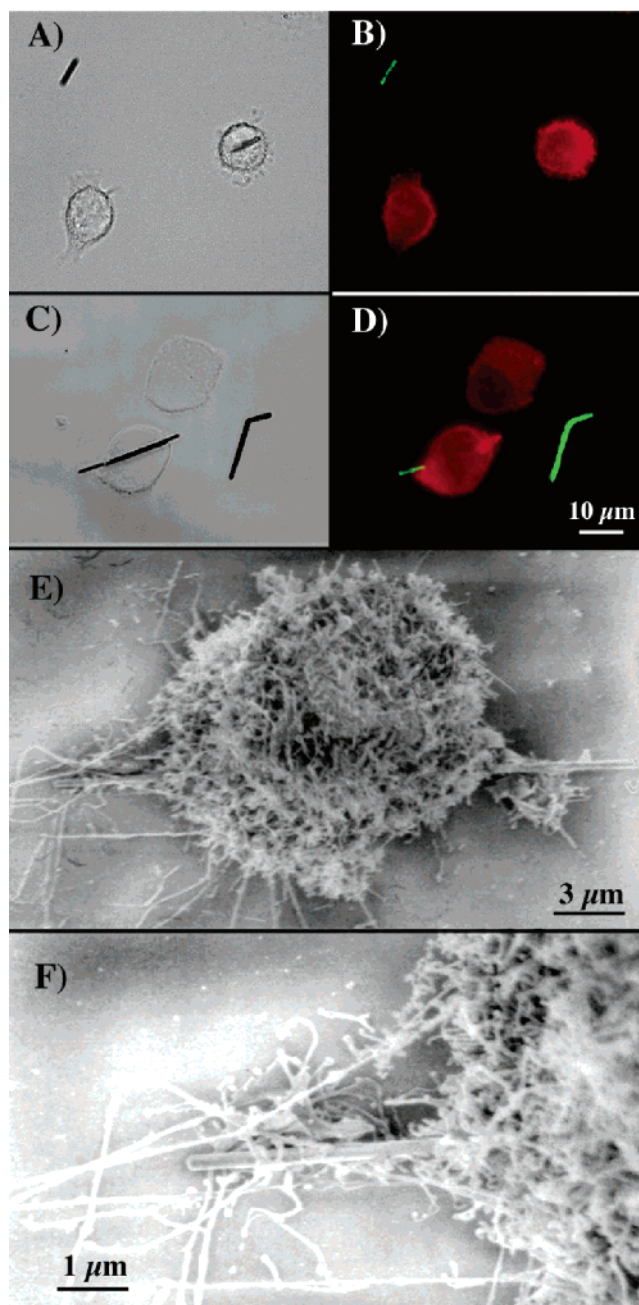


Figure 5. Optical images of suspended 3T3 cells. Top row: suspended cell bound to a 9- μm mouse IgG coated nanowire. (A) Transmitted light and (B) composite fluorescence image of the same cell showing actin filaments (red) and staining of the mouse IgG (green) on an isolated nanowire (upper left) but not on the bound nanowire that is in the cell. Second row: suspended cell bound to a 22- μm mouse IgG coated nanowire. (C) Transmitted light and (D) composite fluorescence image of the same cell showing actin filaments (red) and staining of the mouse IgG on both the portion of the nanowire that is no longer internal to the cell and on an isolated nanowire (right). Bottom row: (E) SEM images of a suspended cell bound to a 22- μm nanowire and (F) detail of the left end of the nanowire shown in (E).

cells were cultured to larger sizes by using the chemotherapeutic agent Mitomycin-C (MitoC) (21, 22). The distributions of cell diameters were measured with a Beckman Z2 Coulter Counter both before and after exposure to MitoC and are shown in Figure 6. Initially, the suspended 3T3 cells have an average diameter of $d_0 = 15 \pm 2 \mu\text{m}$. The MitoC-treated cells continued to grow without division such that their average diameter in-

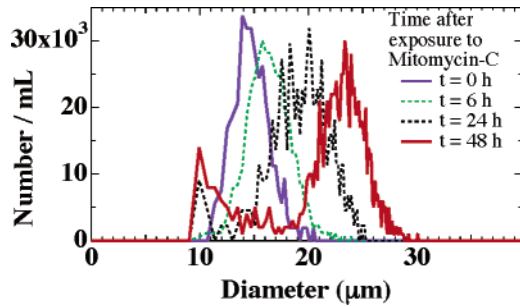


Figure 6. Distribution of cell diameters before and 6, 24, and 48 h after treatment with mitomycin-C. The average cell diameter increases from $d_0 = 15 \mu\text{m}$ to $d_{6\text{h}} = 17 \mu\text{m}$, $d_{24\text{h}} = 20 \mu\text{m}$, and $d_{48\text{h}} = 23 \mu\text{m}$.

creased with time. After 48 h, the average cell diameter increased to $d_{48\text{h}} = 23 \pm 3 \mu\text{m}$. Therefore, we were able to create distinct cell populations with well-separated size distributions. Eventually, the MitoC-treated 3T3 cultures die, with the majority of the cell death occurring after 3 days. At the 48 h time point, only a small fraction had died, which accounts for the tail of smaller diameter objects observed in the Coulter counter data.

Magnetic separations were performed on the 48 h MitoC-treated cells as described above. Results are shown in Figure 7A and B with the results from the normal 3T3 population shown for reference. The purity of the captured cell populations showed similar results as the untreated cells, but we found that the peak in the percent yield shifted from the 15- μm nanowires to the 22- μm nanowires. For both populations, the percent yield is maximized when the nanowire length is equal to the cell diameter, and the maximum yield is about four times larger than the yield achieved using the beads.

These results suggest that cells could be separated on the basis of the size of the cells alone, without the use of specific binding techniques. To demonstrate this possibility directly, we created a heterogeneous population of MitoC-treated and untreated 3T3 cells and performed magnetic separations using 9-, 15-, and 22- μm nanowires. Figure 8A and B show the initial and captured populations for a separation using 22- μm nanowires. Figure 8C shows the percent yield of both the treated and untreated cells in the heterogeneous cell culture, demonstrating that by using the nanowires with the same length as the larger cell diameter, we can preferentially separate out the large cells from the culture. As shown in Figure 8C, using 22- μm nanowires, there is a 71% yield of the large cells and only a 36% yield of the smaller cells. Thus, a culture with an initial ratio of large to small cells of 1:1 will be improved to 5:3 after one separation.

Conclusions

For both the MitoC-treated and untreated cell populations, we observe a general increase in yield for nanowire lengths up to the average cell diameter. One factor that contributes to this is that the magnetic moment of the nanowires is directly proportional to their length. Thus, the force exerted by the magnetic field on the nanowires during the separation increases with the length of the nanowire while the hydrodynamic drag on the cells moving through the culture medium remains constant. Therefore, by using longer nanowires, the captured cells are more strongly held by the magnets during removal of the uncaptured cells from the separator. Also, the doubling of the captured cell purity as length, L , increases from 5 to 15 μm indicates that fewer cells are detaching from the longer nanowires post-capture. This implies that

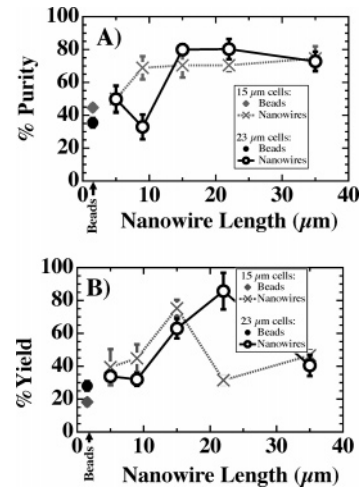


Figure 7. (A) Percent purity versus nanowire length and (B) percent yield versus nanowire length for separations using 23- μm diameter cells (results for 15- μm diameter cells shown as reference).

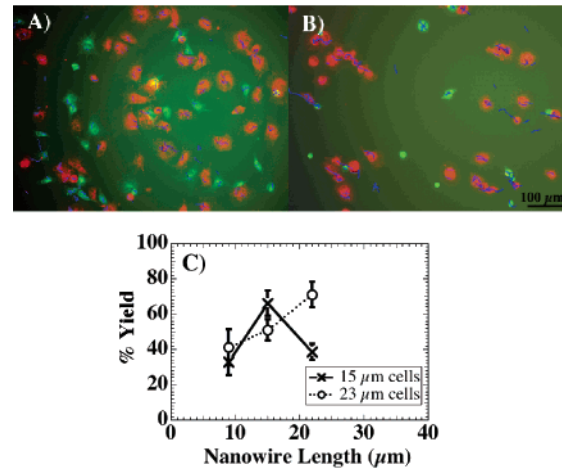


Figure 8. Magnetic separation of heterogeneous cell culture using 22- μm nanowires. The mitomycin-C-treated cells (average diameter = 23 μm) are stained red, the untreated cells (average diameter = 15 μm) are stained green, and nanowires are highlighted in blue. (A) Initial population, (B) captured cell population, and (C) percent yield versus nanowire length of separations of heterogeneous cultures of 15- and 23- μm diameter cells.

the strength of the cell–nanowire binding is increasing for nanowires in this length range. Thus, the increase in yield is likely a combination of both of these effects, although whether the stronger binding is purely due to the increase in surface area or to a more complicated mechanism remains to be determined. When L exceeds the diameter of the suspended cell, the spherical cell can no longer extend along the length of the nanowire. The exposed section of nanowire protruding from the cell will then be more susceptible to influences of mechanical stresses and hence more easily disengaged from the cell. Note, however, that the high purity of the captured populations at large L implies that such detachment occurs early in the separation process. Like beads and other particles, the nanowires are bound and internalized through integrin receptors. Interestingly, unlike spherical particles, these nanowires appear to escape phagocytic endosomes and enter the cytoplasmic compartment. The mechanism by which this escape occurs remains unknown, although our results are consistent with recent observations that nanowires, when bound to DNA plas-

mids, are able to mediate cell transfection, presumably by bringing the plasmids to the cytoplasmic compartment (15). Both the unusual trafficking properties of internalized nanowires and the long nanowires' escape from cells during suspension suggest that these high aspect ratio particles may invoke new mechanisms of cell-particle interactions. Further investigation of the nanowire-cell binding is required to address these mechanisms in detail.

Thus, we have found that the nanowires can achieve high purity of the captured cell population while maintaining high yields in a single-step separation. We also found that this yield can be enhanced by matching the length of the nanowires to the average diameter of the suspended cells. One route to further optimization of cell manipulation with nanowires is the development of cell-specific functionalization of the nanowire surfaces, but our results also suggest the possibility of magnetically separating heterogeneous populations based on differences in cell size alone, without relying on specific binding or other immunomagnetic techniques.

Acknowledgment

This work was supported by DARPA/AFOSR Grant F49620-02-1-0307; by the David and Lucile Packard Foundation through Grant 2001-17715; and by NSF Grant DMR-0080031. TEM images were taken at the Integrated Imaging Center at Johns Hopkins University.

References and Notes

- (1) Maroudas, N. G.; O'Neill, C. H.; Stanton, M. F. Fibroblast Anchorage in Carcinogenesis by Fibers. *Lancet* **1973**, *7807*, 807-809.
- (2) Mossmann, B. T. Carcinogenic Potential of Asbestos and Nonasbestos Fibers. *Environ. Carcinog. Rev.* **1988**, *6*, 151-195.
- (3) Wang, N.; Butler, J. P.; Ingber, D. E. Mechanotransduction Across the Cell Surface and Through the Cytoskeleton. *Science* **1993**, *260*, 1124-1227.
- (4) *Scientific and Clinical Applications of Magnetic Microspheres*; Häfeli, U., Schütt, W., Teller, J., Zborowski, M., Eds.; Plenum Press: New York, 1997.
- (5) Safarik, I.; Safarikova, M. Use of Magnetic Techniques for the Isolation of Cells. *J. Chromatogr. B* **1999**, *722*, 33-53.
- (6) Plank, C.; Schillinger, U.; Scherer, F.; Bergemann, C.; Remy, J.-S.; Krötz, F.; Anton, M.; Lausier, J.; Rosenecker, J. The Magnetofection Method: Using Magnetic Forces to Enhance Gene Delivery. *Biol. Chem.* **2003**, *384*, 737-749.
- (7) Karumanchi, R. S. M. S.; Doddamane, S. N.; Sampangi, C.; Todd, P. W. Field-Assisted Extraction of Cells, Particles and Macromolecules. *Trends Biotechnol.* **2002**, *20*, 72-78.
- (8) Fert, A.; Piroux, L. Magnetic Nanowires. *J. Magn. Magn. Mater.* **1999**, *200*, 338-358.
- (9) Chen, M.; Sun, L.; Bonevitch, J. E.; Reich, D. H.; Chien, C. L.; Searson, P. C. Tuning the Response of Magnetic Suspensions. *Appl. Phys. Lett.* **2003**, *82*, 3310-3312.
- (10) Diggle, J. W.; Downie, T. C.; Goulding, C. W. Anodic Oxide Films on Aluminum. *Chem. Rev.* **1969**, *69*, 365-405.
- (11) Martin, C. R. Nanomaterials: A Membrane-Based Synthetic Approach. *Science* **1994**, *266*, 1961-1966.
- (12) Sun, L.; Searson, P. C.; Chien, C. L. Electrochemical Deposition of Nickel Nanowire Arrays in Single-Crystal Mica Films. *Appl. Phys. Lett.* **1999**, *74*, 2803-2805.
- (13) Bauer, L. A.; Reich, D. H.; Meyer, G. J. Selective Functionalization of Two-Component Magnetic Nanowires. *Langmuir* **2003**, *19*, 7043-7048.
- (14) Birenbaum, N.; Lai, B. T.; Chen, C. S.; Reich, D. H.; Meyer, G. J. Selective Noncovalent Adsorption of Protein to Bifunctional Metallic Nanowire Surfaces. *Langmuir* **2003**, *19*, 9580-9582.
- (15) Salem, A. K.; Searson, P. C.; Leong, K. W. Multifunctional Nanorods for Gene Delivery. *Nat. Mater.* **2003**, *2*, 668-671.
- (16) Hultgren, A.; Tanase, M.; Chen, C. S.; Meyer, G. J.; Reich, D. H. Cell Manipulation using Magnetic Nanowires. *J. Appl. Phys.* **2003**, *93*, 7554-7556.
- (17) Tanase, M.; Bauer, L. A.; Hultgren, A.; Silevitch, D. M.; Sun, L.; Reich, D. H.; Searson, P. C.; Meyer, G. J. Magnetic Alignment of Fluorescent Nanowires. *Nanoletters* **2001**, *1*, 155-158.
- (18) Vassiliou, J. K.; Mehrotra, V.; Otto, J. W.; Dollahon, N. R. Optical Absorption Tail and Superparamagnetism of γ -Fe₂O₃. *Mater. Sci. Forum* **1996**, *225*, 725-733.
- (19) Allen, L.-A. H.; Aderem, A. Molecular Definition of Distinct Cytoskeletal Structures Involved in Complement- and Fc Receptor-Mediated Phagocytosis in Macrophages. *J. Exp. Med.* **1996**, *184*, 627-637.
- (20) Tjelle, T. E.; Lovdal, T.; Berg, T. Phagosome Dynamics and Function. *BioEssays* **2000**, *22*, 255-263.
- (21) Rheinwald, J. G. Serial Cultivation of Normal Human Epidermal Keratinocytes. *Methods Cell Biol.* **1980**, *21A*, 229-254.
- (22) Bhatia, S. N.; Balis, U. J.; Yarmush, M. L.; Toner, M. Microfabrication of Hepatocyte/Fibroblast Co-cultures: Role of Homotypic Cell Interactions. *Biotechnol. Prog.* **1998**, *14*, 378-387.

Accepted for publication October 20, 2004.

BP049734W